Article:
Liu, S., Wang, Y., Qin, N. orcid.org/0000-0002-6437-9027 et al. (1 more author) (2019) Quantification of airfoil aerodynamic uncertainty due to pressure-sensitive paint thickness. AIAA Journal. ISSN 0001-1452

https://doi.org/10.2514/1.j058801

Quantification of Airfoil Aerodynamic Uncertainty due to thickness effect of pressure sensitive paint

Siyang Liu,[1] and Yibin Wang.[2]
Nanjing University of Aeronautics and Astronautics, Nanjing 210016, China

Ning Qin [3]
University of Sheffield, Sheffield S1 3JD, UK

and
Ning Zhao [4]
Nanjing University of Aeronautics and Astronautics, Nanjing 210016, China

In this paper, uncertainty quantification is used to investigate the propagation of the uncertainty of the pressure sensitive paint (PSP) thickness distribution to the uncertainty of aerodynamic force measured. Specifically, airfoil surface pressure coefficient (C_p) and aerodynamic lift coefficient (C_l) of a natural laminar flow (NLF) wing are analyzed with uncertain PSP thickness distribution. The airfoil with PSP applied is parameterized by using a novel parameterization method based on radial basis function interpolation. As a characteristic of wing aerodynamic performance, C_l is determined by surface pressure distribution which can be affected by uncertainties of PSP binder thickness. A Kriging response surface method has been used to develop a surrogate model to represent the RANS solution of the flow around the airfoil with PSP. This enables the use of Monte Carlo simulations to obtain stochastic output, including the probability of the occurrence of significantly inaccurate output values affected by the inputs

[1] PhD student, College of Aerospace Engineering.

[2] Lecturer, College of Aerospace Engineering.

[3] Professor of Aerodynamics, Department of Mechanical Engineering, AIAA Associate Fellow.

[4] Professor, College of Aerospace Engineering.

subjecting to Gaussian distributions. An error margin and associated probability for its occurrence are recommended to account for uncertainties for the aerodynamic force occurring in the PSP measurement.

Nomenclature

C_l	=	lift coefficient
C_p	=	pressure coefficient
$C_{l,o}$	=	lift coefficient of original airfoil without PSP
$C_{p,o}$	=	pressure coefficient of original airfoil without PSP
$C_{p,E}$	=	the expected value of pressure coefficient
$C_{l,E}$	=	the expected value of lift coefficient
CoV	=	coefficient of variation
COV	=	covariance
D_ω	=	the cross-diffusion term
E	=	total energy
$E_{\gamma 1}$	=	transition source
$E_{\gamma 2}$	=	destruction/ relaminarization sources
F	=	regression process
F	=	flux vector
G_k	=	production of turbulence kinetic energy
G_ω	=	generation of ω
MCM	=	Monte Carlo method
NFL	=	natural laminar flow

P	=	probability
p_X	=	probability density function
P_X	=	cumulative density function
PDF	=	probability density function
PSP	=	pressure sensitive paint
PT	=	pressure tap
$P_{\gamma 1}$	=	transition source
$P_{\gamma 2}$	=	destruction/ relaminarization sources
Q	=	vector of conserved variables
q	=	heat flux
R	=	correlation model
RANS	=	Reynolds-average Navier-Stoles equations
RBF	=	radial basis function
$Re_{\theta t}$	=	the transition momentum thickness Reynolds number
RSM	=	response surface method
$S_{k,\omega}$	=	source terms
UQ	=	uncertainty quantification
u, v, ω	=	Cartesian velocity components
x	=	x and y coordinates
x_c	=	original coordinates of the boundary nodes
x_b, y_b	=	coordinates of base line geometry
x_{cj}, y_{cj}	=	control nodes of the interpolation

$Y_{k,\omega}$ = dissipation due to turbulence

β = regression parameter

β_k = control nodes

β^* = process coefficient

$\Gamma_{k,\omega}$ = effective diffusivity

γ = intermittency

γ- Re_θ = transition SST model (4-equations model)

Φ = radial basis function

σ = standard deviation

σ^2 = variance

μ = expected value (mean)

ρ = flow density

τ = stress tensor

Subscripts

k = number of control nodes

o = original geometry without PSP

E = expected value

I. Introduction

Wind tunnel tests involve measurements of flow properties, such as pressure, temperature, density, velocity, and forces and moments exerted on an object. Some of the measurements possess certain level of intrusion to the flow field and others may cause small geometrical changes that are not negligible.

Pressure sensitive paint (PSP) has been used in experimental aerodynamics since the 1990s for measuring the surface pressure through oxygen concentration [1]. It utilizes the photoluminescence and oxygen quenching effect to build up the correspondence between luminescent intensity and surface pressure distribution. PSP has becoming popular as it can provide more detailed and continuous pressure distribution data on aerodynamic surfaces as compared to the conventional pressure taps (PT). It has become a useful technique for experimental research for varied aerodynamic problems, and has been widely used in transonic flows, hypersonic flows, low-speed flows, and transient flows [2]-[5]. PSP measurements can be categorized by types of binder materials with different thickness. For AA-PSP (anodized aluminum pressure-sensitive paint) measurement, the thickness can vary from 10-30μm. PC-PSP (porous polymer/ceramic pressure-sensitive paint) normally has a thickness of 50μm. The thickness of conventional PSP (Polymer PSP) and TLC-PSP (thin-layer chromatography pressure-sensitive paint) are 60 and 152μm [6]. The thickness uncertainty may affect response time and the obtained results. Many studies have been carried out to assess the sources of uncertainty in PSP measurement, such as pixel-based and camera-based uncertainties, luminescent light intensity, surface temperature [7][8].

Hubner et al. [9] investigated the influence of PSP coating to the response time for a thin paint, where pressure features of short-duration, transient flow were measured in a shock tube. The difference between the data of PSP measurement and that of the transducer was found to range up to 5%. Liu et al. [10] applied a Joukowsky airfoil in subsonic flow to perform a complete sensitivity analysis of PSP measurement uncertainty for various systems including paint, photodetector, optical filters, and illumination sources. Due to aerodynamic loads, the paint thickness displacements cause the spatial luminescent intensity change. These studies regarding the PSP thickness have been so far limited to response time shift and luminescent

intensity. From the literature, there has so far no detailed study on the thickness uncertainty due to PSP measurement on aerodynamic performance.

In the present paper, uncertainty quantification is employed to investigate effects of paint thickness on aerodynamic performance in PSP measurement. As the distribution of these features are aleatory, the analysis of the uncertainty associated to the features is also required.

Uncertainty Quantification (UQ) is often considered as a method to give the error bars added to the high fidelity CFD predictions [11]. There are varied uncertainty quantification approaches such as Polynomial Chaos method, sensitivity analysis approach, Monte Carlo method, surrogate model approach [12], etc. Bunker [15] carried out a study of uncertainty of geometrical and operational variations for highly cooled turbine blades by Monte Carlo simulation. Montomoli and Massini [16] carried out Monte Carlo simulation with surrogate model to investigate the impact of "Black Swan" event on compressor stator hot gas ingestion. The reliability of various conventional UQ methods was assessed for its limits in including the "Black Swan" event prediction. Monte Carlo simulation with surrogate model approach was found to be efficient and accurate with large amount of realizations. In the present study, Monte Carlo simulations with a surrogate model are applied to quantify uncertainties within PSP paint thickness.

II.Flow field computation method and validation

Recently, an experimental study of an NLF wing at a transonic condition was conducted, for which both PT and PSP were used [17]. In this experimental study the NLF wing is a 20 sweep back wing. The stream wise aligned airfoil of the wing is a RAE5243 airfoil. The maximum thickness is 11% of the chord [17]. Figure 1 shows the surface pressure distribution in the central section of the wing from the computation by SST γ- Re_θ model and the experiments by PT and PSP [17]. Figure 2 shows the intermittency factor distribution for the central section of the wing. The steep increase in the intermittency factor gives the location of transition onset which is around 0.56 of the chord. It can be seen that the pressure

coefficient obtained by PT and numerical computation shows a good agreement at the mid-span upper surface of the wing. The computation was conducted with a Mach number of 0.75 and an angle of attack of 3 degree. A difference between measured PSP results and PT results can be observed at mid-span upper surface. As conventional techniques, both PT and PSP have been widely used in wind tunnel tests as robust measuring techniques and have been well validated. Considering the uncertainty for the paint or binder thickness between 10-152μm may have caused the difference. Despite the small dimension, the airfoil shape deviations may still have some significant impact on aerodynamic performance (lift and drag) of the wing. The deviation of results from PSP to PT experiment may be attributed to the uncertain PSP binder thickness.

The aim of this study is to investigate the geometric thickness effect occurring in PSP measurement and provide calibration margin if necessary. In this study, the pressure coefficient and lift coefficient of a wind tunnel airfoil model with pressure sensitive paint were investigated using uncertainty quantification. In order to achieve the aim of UQ of airfoil with PSP, a novel parameterization method based on radial basis function interpolation is proposed first. To carry out MCM analysis for UQ, a Kriging Response surface surrogate model has been developed to deal with the large computational demand of MCM.

The governing equations used in this study are compressible Navier-Stokes equations.

$$\frac{\partial}{\partial \mathrm{t}} \iiint_{\Omega} \mathbf{Q} \mathrm{dV} + \iiint_{\partial \Omega} \mathbf{F} \cdot \mathrm{ndS} = 0 \tag{1}$$

where Ω stands for the bounded domain. **Q** is the vector of conserved variables and **F** is the flux vector. **Q** and **F** are given by

$$\mathbf{Q} = \begin{pmatrix} \rho & \rho \mathrm{u} & \rho \mathrm{v} & \rho \omega & \rho \mathrm{E} \end{pmatrix}^{\mathrm{T}} \tag{2}$$

$$\mathbf{F} = \begin{pmatrix} \mathbf{F}_{\mathrm{i}} & \mathbf{F}_{\mathrm{j}} & \mathbf{F}_{\mathrm{k}} \end{pmatrix}^{\mathrm{T}} \tag{3}$$

where ρ is the flow density, u, v, ω are velocity components in three Cartesian directions. E is the total energy. **F** is expressed in three directions:

$$\mathbf{F}_x = \begin{bmatrix} \rho u \\ \rho u^2 + p - \tau_{xx} \\ \rho uv - \tau_{xy} \\ \rho uw - \tau_{xz} \\ u(\rho E + p) - u\tau_{xx} - v\tau_{xy} - w\tau_{xz} - q_x \end{bmatrix} \tag{4}$$

$$\mathbf{F}_y = \begin{bmatrix} \rho v \\ \rho vu - \tau_{yx} \\ \rho v^2 - \tau_{yy} \\ \rho vw - \tau_{yz} \\ v(\rho E + p) - u\tau_{yx} - v\tau_{yy} - w\tau_{yz} - q_y \end{bmatrix} \tag{5}$$

$$\mathbf{F}_z = \begin{bmatrix} \rho w \\ \rho wu - \tau_{zx} \\ \rho wv - \tau_{zy} \\ \rho w^2 + p - \tau_{zz} \\ w(\rho E + p) - u\tau_{zx} - v\tau_{zy} - w\tau_{zz} - q_z \end{bmatrix} \tag{6}$$

where p is the static pressure, τ is the stress tensor and q is the heat flux.

The transition SST model was used to tackle the NLF wing and airfoil. It is based on the coupling of the SST k-ω transport equations with one intermittency transport equation and one transition onset criteria equation. The SST k-ω transport equations are:

$$\frac{\partial}{\partial t}(\rho k) + \frac{\partial}{\partial x_i}(\rho k u_i) = \frac{\partial}{\partial x_j}\left(\Gamma_k \frac{\partial k}{\partial x_j}\right) + G_k - Y_k + S_k \tag{7}$$

$$\frac{\partial}{\partial t}(\rho \omega) + \frac{\partial}{\partial x_j}(\rho \omega u_j) = \frac{\partial}{\partial x_j}\left(\Gamma_\omega \frac{\partial \omega}{\partial x_j}\right) + G_\omega - Y_\omega + S_\omega + D_\omega \tag{8}$$

where G_k stands for the production of turbulence kinetic energy. G_ω stands for the generation of ω. Γ_k and Γ_ω are the effective diffusivity of k and ω. Y_k and Y_ω are the dissipation of k and ω due to turbulence. S_k and S_ω are source terms, and D_ω stands for the cross-diffusion term.

The transport equation for the intermittency γ is:

$$\frac{\partial(\rho\gamma)}{\partial t} + \frac{\partial(\rho U_j \gamma)}{\partial x_j} = P_{\gamma 1} - E_{\gamma 1} + P_{\gamma 2} - E_{\gamma 2} + \frac{\partial}{\partial x_j}\left[\left(\mu + \frac{\mu_t}{\sigma_\gamma}\right)\frac{\partial \gamma}{\partial x_j}\right] \tag{9}$$

where $P_{\gamma 1}$ and $E_{\gamma 1}$ are the transition sources, and $P_{\gamma 2}$ and $E_{\gamma 2}$ are the destruction/relaminarization sources.

The transport equation for the transition momentum thickness Reynolds number $Re_{\theta t}$ is:

$$\frac{\partial\left(\rho \mathrm{Re}_{\theta t}\right)}{\partial t}+\frac{\partial\left(\rho \mathrm{U}_{\mathrm{j}} \mathrm{Re}_{\theta t}\right)}{\partial \mathrm{x}_{\mathrm{j}}}=\mathrm{P}_{\theta t}+\frac{\partial}{\partial \mathrm{x}_{\mathrm{j}}}\left[\left(\mu+\mu_{t}\right)\frac{\partial \mathrm{Re}_{\theta t}}{\partial \mathrm{x}_{\mathrm{j}}}\right] \tag{10}$$

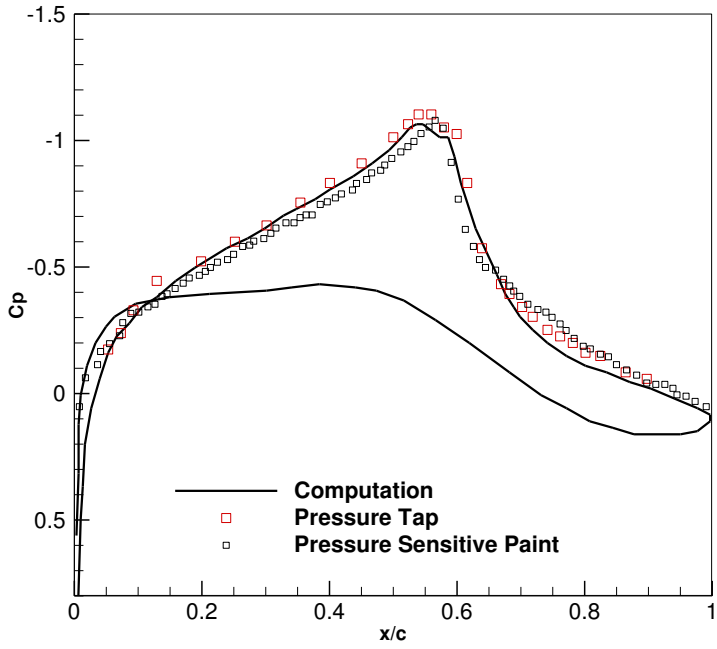

Fig. 1 Pressure coefficient distribution for PT, PSP and Computation [17]

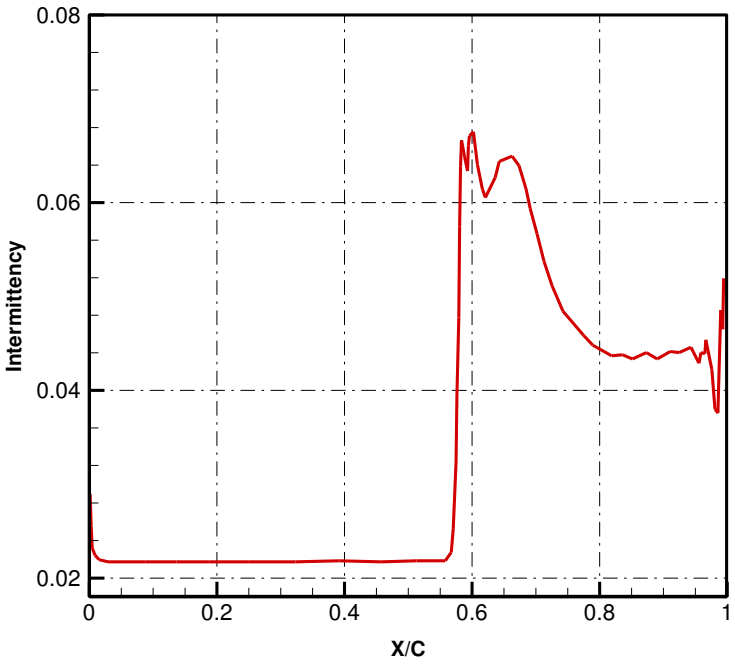

Fig. 2 Intermittency factor distribution for computational result

III. RBF Parameterization for airfoil with PSP

The wind tunnel tests indicated PSP can potentially has some significant effects on the pressure distribution and therefore the aerodynamic force. This is believed to come from the alternation of the aerodynamic surface due to PSP. However, this alternation is non-uniform, unquantified and therefore uncertain. In order to investigate the proposed problem, the RAE5243 airfoil for a max thickness of 11% chord with PSP which is consistent with the Ref. [17] was considered.

As PSP normally has a thickness between 10-152μm, an appropriate parameterization method for the wind tunnel airfoil with PSP painted on is required. A parameterization method [19] is developed based on the radial basis function interpolation [20]. This method is used to represent the desired airfoil with paint thickness properly with a small number of uncertain parameters and can also present small deviations of the airfoil by altering the design variables.

For different geometries with small variations, either deforming mesh method or re-meshing method can be used to obtain the new mesh. Both methods require additional computational cost. The RBF parameterization method can generate mesh with altered surface directly from the design variables which can effectively increase the efficiency of the process. Therefore, for a series of slightly deformed geometries, a set of meshes can be created along with the parametrization process directly.

For a radial basis function, the value of the function only depends on the distance from the reference point called the radial center. It can be described as:

$$\phi(\mathbf{x}) = \phi(\|\mathbf{x}\|) \tag{11}$$

The chosen radial basis function is the Wend land's C2 function: $\phi(\xi) = (1 - \xi)^4(4\xi + 1)$.

The baseline displacement function transformation utilizes the following:

$$y = y_b + \alpha A \tag{12}$$

$$x = x_b \tag{13}$$

$$A_i = \phi\left(\sqrt{\left(x_b - x_{cj}\right)^2 + \left(y_b - y_{cj}\right)^2}\right) \tag{14}$$

$$\alpha = (y_c - y_b)M^{-1} \tag{15}$$

$$M_{ij} = \phi\left(\sqrt{\left(x_{ci} - x_{cj}\right)^2 + \left(y_{ci} - y_{cj}\right)^2}\right) \tag{16}$$

where x and y are the x and y coordinates for the new geometries; $x_b$and y_b are the coordinates for baseline geometries; x_{ci}, y_{ci} and x_{cj}, y_{cj} are the control nodes of the interpolation. The first term in Eq. (12) on the right is baseline function which represents the original configuration of the airfoil or the baseline geometry, the second term on the right is the displacement function which describes the displacement of interior mesh node. The displacement of the interior mesh node can be obtained by computing displacement of geometry boundary node from Eq. (5,6).

As shown in Fig. 3, a greedy algorithm [18] has been implemented for reducing the control points before the simulation. The interpolation error for 63 natural laminar flow airfoils with different number of control points have been compared to verify the selected control points on the geometries for constructing the matrix, as shown in Fig. 4. In addition, the matrix of the Radial Basis function interpolation for geometric deformation and mesh motion is the same. Therefore, the mesh deformation can be computed directly from the matrix along with the geometric deformation with high efficiency. Current approach directly defines the geometry, thus there is no interpolation error.

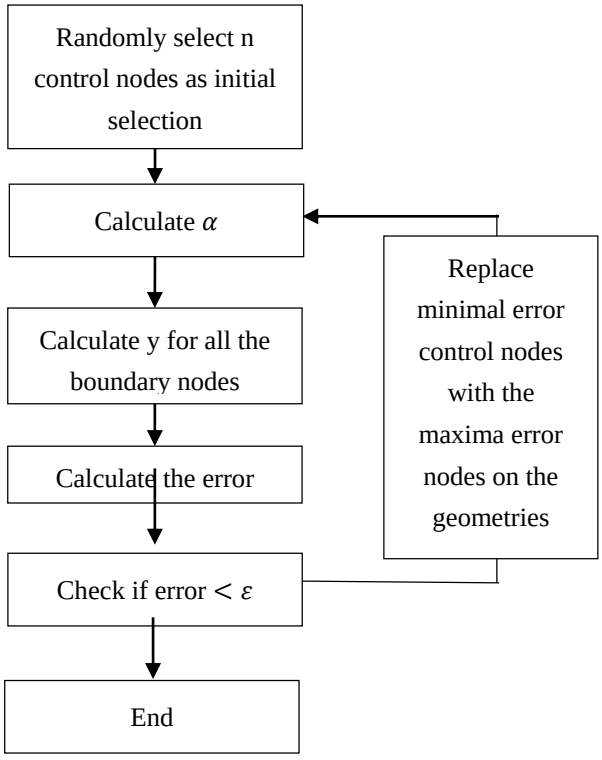

Fig. 3 Flow chart of greedy algorithm

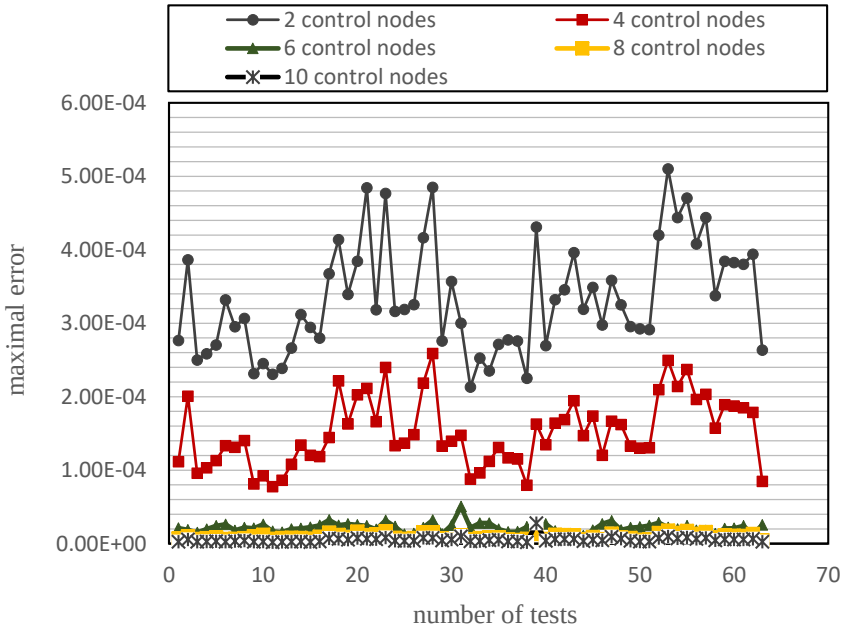

Fig. 4 Geometric inverse fitting test and results

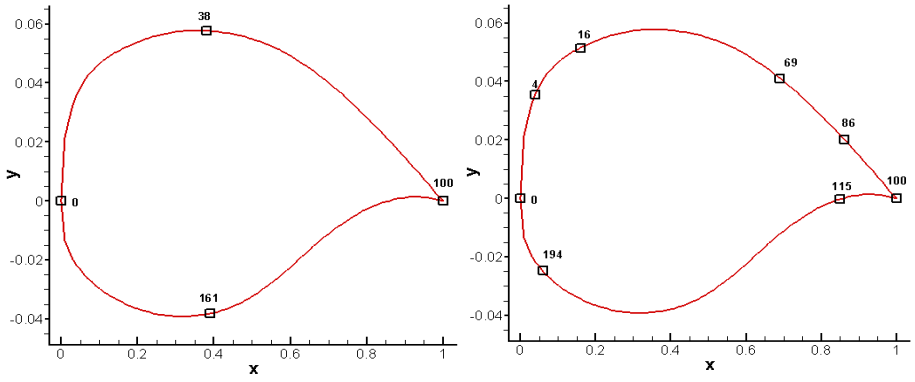

(a) Two control nodes (b) Six control nodes

Fig. 5 Distribution of control nodes

Table 1 Positions of 6 control points

x position	0.0372	0.1581	0.6884	0.8627	0.0848	0.0605
y position	0.0352	0.0517	0.0410	0.0201	-0.0002	-0.0249

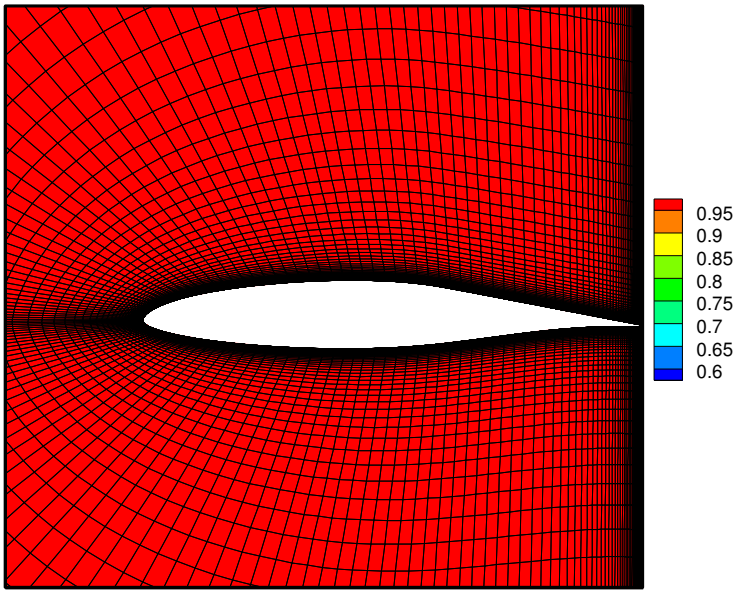

Fig. 6 Mesh quality

Table 2: Grid convergence

Mesh nodes	10000	20000	30000	40000	50000
C_l	0.6609	0.6497	0.6424	0.6415	0.6414

In order to validate the RBF parameterization method, a geometric inverse fitting process has been carried out by comparing a wide range of original airfoils with the RBF representation. The maximum error represents the maximum displacement from the parameterized airfoil to its original airfoil. The tolerance for wind tunnel geometries, 5×10^{-4} relative to the chord length, is employed as the criteria to exam the fitting accuracy [19]. Fig. 4 shows the geometric inverse fitting test and the results by the RBF method. The errors reach 2×10^{-5} when the number of control nodes increases from 2 to 10. Fig. 5 shows the distributions of control nodes for 2 control nodes and 6 control nodes. In this study, 6 control parameters are applied as the kernels for the RBF parameterization method. A normalized α_n is considered as input design variable subjecting to Gaussian distribution.

The displacement of geometry is $\delta y = y_c - y_b = \alpha M$, thus $\alpha = \delta y M^{-1}$. When α is zero, the geometry obtained is exactly the original airfoil shape. α_{max} can be obtained for a maximum possible paint thickness 152μm. α_{normal} can be

obtained for a normal paint thickness 60μm. $\alpha_{\min}$ can be obtained for a minimum possible thickness 10μm. Instead of directly using α , a normalized $\alpha_{\mathrm{n}} = \dfrac{\alpha}{\alpha_{\mathrm{normal}}}$ is applied as the input design variable to provide a logical way of implementing Gaussian distribution to the inputs. Fig. **6** shows the mesh quality contour for a deformed geometry. The mesh quality metric is based on the study of P.M. Knupp [21]. Table 2 shows the grid convergence. The grid nodes number used in this study is 40000. Fig. 7 shows parameterization of the same airfoil with varied paint thickness distribution. The black lines represent different binder thickness distribution. This non-uniformity of binder thickness represents the painting process and the uncertain coating property itself. The thick red line represents the original airfoil baseline, while the other lines represent airfoils with three random non-uniform binder thickness distributions. The maximum paint binder thickness was no more than 200μm according to the PSP property. By giving a set of appropriate parameters as the input of the RBF parameterization method, the airfoil shape and mesh with a new non-uniform binder thickness distribution can be obtained, and therefore flow simulations can be carried out based on the PSP deformed shapes and the corresponding meshes. Figure Fig. 8 shows the near surface meshes for baseline geometry (thick red line) and one deformed geometry (thick black line).

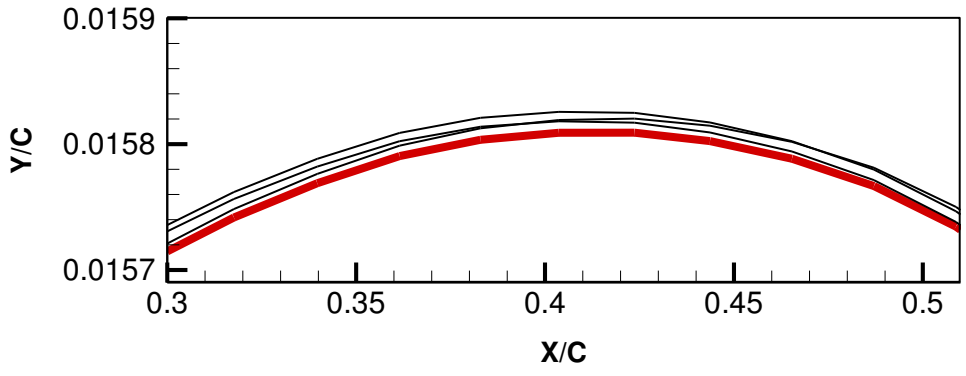

Fig. 7 Airfoil with non-uniform paint thickness (Red-line stands for the airfoil baseline)

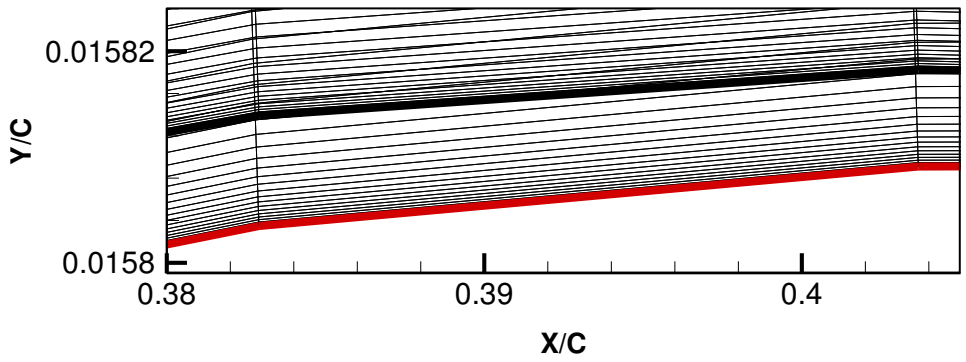

Fig. 8 Mesh deformation near surface

IV.Kriging Surrogate model for airfoil with PSP

In the last section, the parameterization and mesh generation methods have been described for the airfoil with PSP. A standard Monte Carlo simulation method (MCM) is implemented which can give directly the stochastic output and avoid the effect by specific models [16]. The MC method converges to the theoretical solution when the number of realization approaches infinity theoretically. Therefore the larger the number of experiments is, the more accurate the obtained results will be. As the evaluation of the population are carried out by RANS solutions, a large number of realization will lead to severe computation time cost using MCM. Therefore, a surrogate model is proposed here to overcome this problem.

The surrogate model is developed using Kriging interpolation. Kriging interpolation was originally introduced in the geostatistics and mining fields. For example, Yamazaki and Arakawa [22] applied the Kriging response surface approach to shape optimization of vertical-axis wind turbine airfoils. A kriging model provides a way to predict the response of unobserved points based on all of the observed points, and it consists of a global model and local deviations, which is a realization of a Gaussian process governed by prior covariance [23]. In this study, a Kriging approximation based response surface is employed as the surrogate model. The Kriging model contains a regression process F and a random process z.

$$y(x) = F(\beta, x) + z(x) \tag{17}$$

where the coefficient β is the regression parameter. The random process contains the process variance σ^2 and a correlation model R with parameter θ [23].

$$COV[z(\omega)\, z(x)] = \sigma^2 R(\theta, \omega, x) \tag{18}$$

For a design space x $[x_1, x_2, ..., x_n]$ and a response Y $[y_1, y_2, \ldots, y_n]$ the process coefficient β^* can be determined as

$$\beta^* = (F(x)^T\, R^{-1}\, F(x)^T)^{-1}\, F(x)^T R^{-1} Y \tag{19}$$

Therefore, the Kriging predictor can be expressed as:

$$y(x) = f^T \beta^* + r^T R^{-1}(Y - F\,\beta^*) \tag{20}$$

The kriging surrogate model developed here contains a regression model with polynomials and a correlation model. In this case, with 6 input parameters controlling the airfoil PSP painting thickness, about 100 flow simulations are carried out to construct the surrogate model. The turbulence model for the flow solution is the SST γ-Re_θ model, and the Mach number is 0.75.

V.Validation for Kriging Surrogate model

Validations have been carried out for the surrogate model proposed here. Nine sets of parameters have been randomly chosen as inputs for airfoil with different PSP thickness distributions. For each set of parameters, a RANS simulation was

carried out providing the coefficient of pressure (C_p) and lift (C_l) as the outputs. The outputs for the surrogate model of corresponding set of parameters were also obtained and compared with that of the RANS. As shown in Table 3, for 9 random parameter series the differences of pressure coefficient at airfoil maximum height position are generally less than 1.4% compared with RANS results. As shown in Table 4, the differences of lift coefficient from the surrogate model to RANS results are all less than 0.6% for 9 random parameter series. These results show that the Kriging surrogate model have a reasonably good agreement with the RANS result for C_p and C_l. Therefore, the Kriging surrogate model was proved to represent the RANS solutions accurately, and then to be implemented with MCM for UQ of C_p and C_l.

Table 3 Differences of C_p at maximum airfoil thickness from the RANS results

Differences from the RANS solutions for 9 random cases									
RANS (C_p)	-1.293	-1.283	-1.258	-1.269	-1.28	-1.272	-1.244	-1.285	-1.272
Kriging (C_p)	-1.291	-1.273	-1.247	-1.266	-1.277	-1.271	-1.227	-1.269	-1.256
Difference(%)	0.1987	0.7188	0.8615	0.2693	0.2382	0.0381	1.351	1.238	1.242

Table 4 Differences of C_l from the RANS results

Differences from the RANS solutions for 9 random cases									
RANS (C_l)	0.6518	0.6635	0.671	0.66	0.661	0.6471	0.6462	0.6556	0.6356
Kriging (C_l)	0.6514	0.6616	0.6676	0.6589	0.6607	0.6443	0.6438	0.6546	0.6355
Difference(%)	0.061	0.283	0.506	0.166	0.0454	0.423	0.362	0.148	0.0153

VI.Monte Carlo based UQ for C_p with kriging surrogate model at airfoil maximum thickness position

The Monte Carlo methods are stochastic techniques based on the use of random numbers to investigate stochastic problems [24]. The input can be expressed from the expected value and standard deviation (SD) of a random variable:

$$x_i = \mu + \sigma \cdot r_i \tag{21}$$

where r_i is the random value generated with a mean of 0 and an SD of 1 of a Gaussian distribution. For the MCM process, 10^7 samples were implemented here. For each sample, a realization of computation via surrogate model has been

obtained. For the Kriging surrogate model, 100 flow simulation results with 6 parameters as input have been used to construct the surrogate model. 6 input parameters in the Kriging model subjected to Gaussian distribution, shown as

$$\text{Gaussian PDF} = \frac{1}{\sigma\sqrt{2\pi}} e^{-\frac{(x-\mu)^2}{2\sigma^2}} \tag{22}$$

The uncertainty effect was performed in terms of the coefficient of variation (CoV), which is defined as the ratio of standard deviation to the absolute expected value of the variable. According to [24], the CoV for geometric variables has been taken a moderate value of 3% (commonly 1% can be regarded as low, while 5% can be regarded as relatively high). According to previous definition of input variables α_n, the 3-sigma rules [25] and the value of CoV, the input variables are expected to follow a Gaussian distribution with a mean value μ=1 and a standard deviation σ=0.03.

In order to demonstrate that the stochastic output is properly converged [15], the convergence ratio of the moments of the MCM with the surrogate model is shown in Fig. 9. The probability distribution $P_X(C_p)$ of the pressure coefficient at airfoil maximum height point is shown in Fig. 10, where X is the random variable.

The pressure coefficient of original airfoil without PSP paint obtained by flow solutions is $C_{p,o}$= -1.293. The expected value of pressure coefficient obtained by surrogate model is $C_{p,E}$= -1.2742. The standard deviation converges to 0.0078; the skewness to -0.025; and the kurtosis to 3.02. The coefficient of variation for pressure coefficient CoV_p=0.6%.

In Fig. 11 the cumulative distribution $P_X(C_p)$ for C_p with deviation was plotted, where $P_X(C_p)=\int p_X(C_p)\mathrm{d}(C_p)$. The deviation is the difference between obtained C_p and the expected value which is also the deterministic baseline value of the obtained results. The probability of obtaining a C_p less than -1.291 is 1%. The probability of obtaining a C_p less than -1.2756 is 50%. The probability of obtaining a C_p less than -1.261 is 99%. Therefore, the chance of having a C_p less than -1.291 or greater than -1.261 is 1% which can be regarded as a rare event. The corresponding lower and upper bonds for deviations are respectively 0.0168 and 0.0136.

Therefore, under the effect of PSP paint binder thickness, the pressure coefficient at airfoil maximum thickness position increased from -1.293 to -1.2742. Moreover, due to the paint's randomness and non-uniformity, the captured C_p ranged from $C_{p,E}$ -0.0168 to $C_{p,E}$ $+0.0136$.

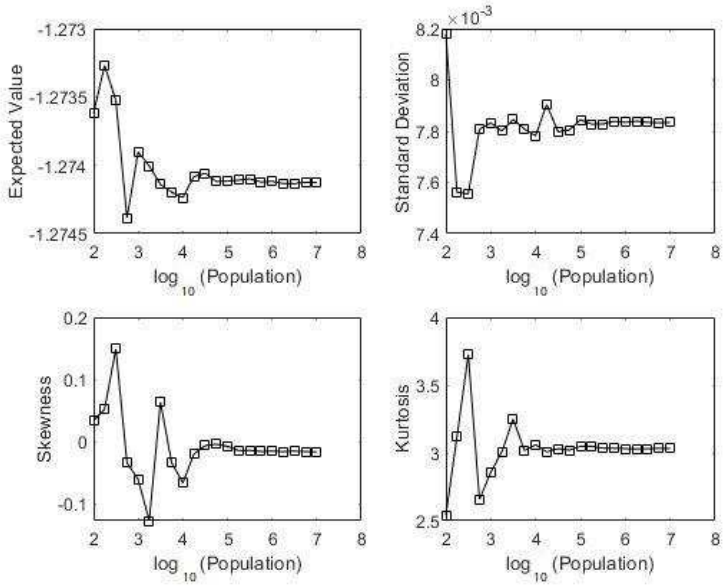

Fig. 9 Convergence of four moments for C_p at airfoil maximum height

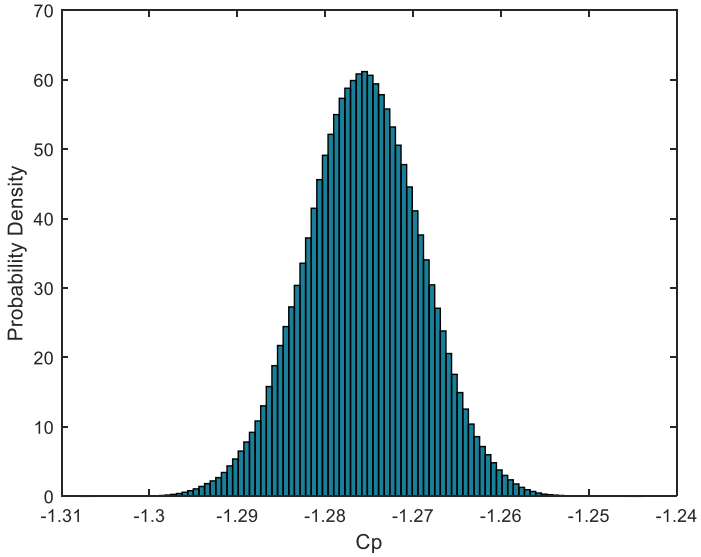

Fig. 10 Probability distribution for C_p at airfoil maximum height

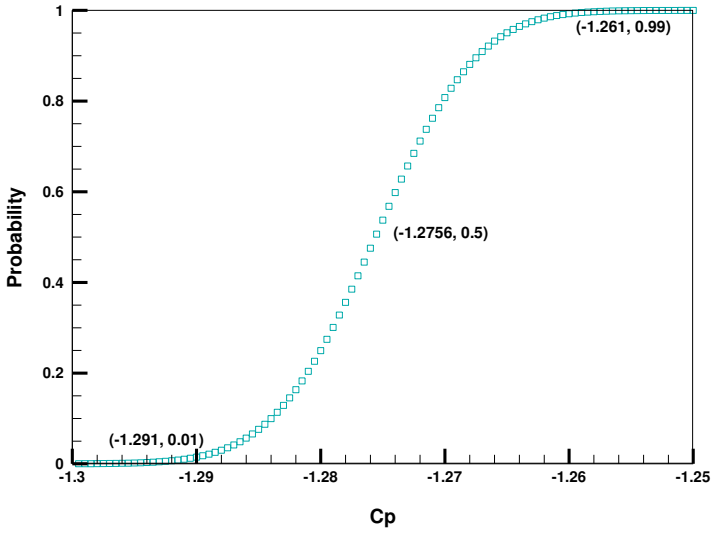

Fig. 11 Probability of cumulative distribution for pressure coefficient with deviation

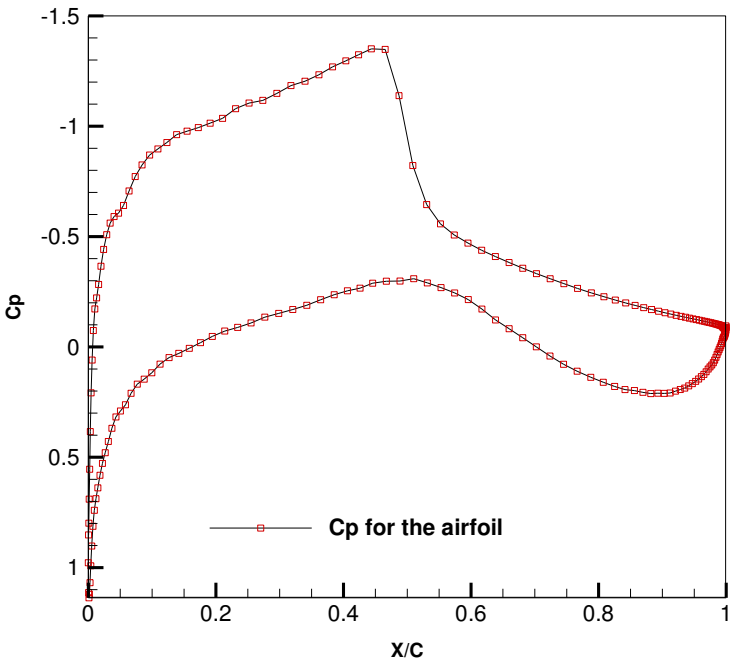

Fig. 12 Pressure coefficient distribution for the base line airfoil

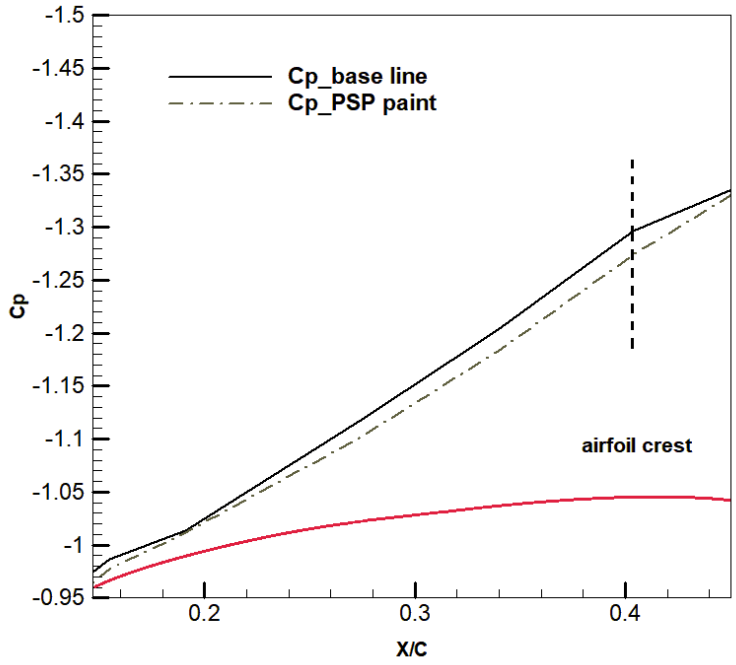

Fig. 13 Pressure coefficient distribution for airfoil base line and airfoil with PSP (Red-line stands for the airfoil shape)

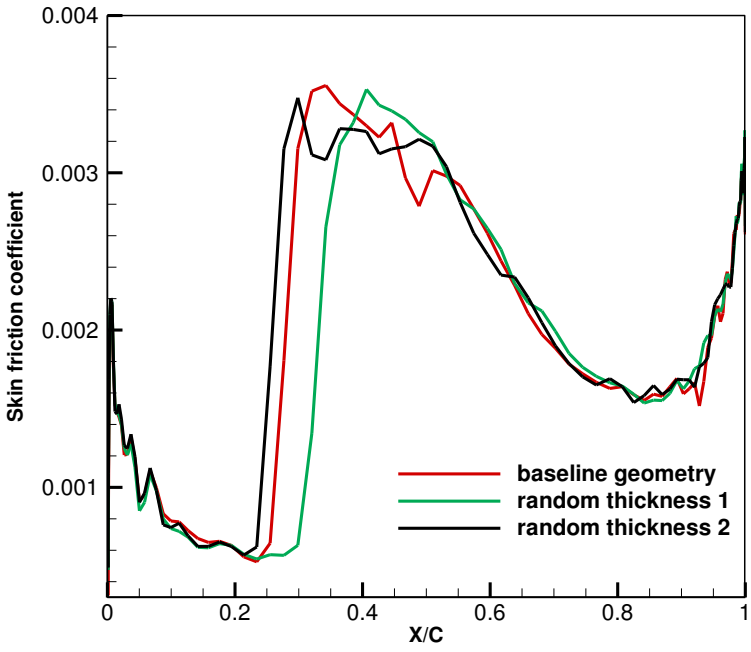

Fig. 14 Skin friction coefficient distribution baseline geometry and two cases with random paint thickness distribution

FigureFig. 12 shows the pressure coefficient distribution for the base line airfoil. In order to obtain the pressure coefficient distribution along the upper surface of the airfoil with the effect of paint thickness, surrogate model with MCM has been implemented for several positions along the chord. Fig. 13 shows the comparison of pressure coefficient before the shock between airfoil base line and airfoil with PSP. The red-line represents the airfoil shape. Compared to experimental result (Fig. 1), a similar trend has been observed where the pressure coefficient distribution with PSP before the shock is generally lower than that of the airfoil baseline. Fig. 14 shows the skin friction coefficient distribution for the baseline geometry case and two random paint thickness distribution cases. The steep increase of skin friction coefficient indicates the transition onset position. From the figure we can see that the paint thickness uncertainties can also affect the transition onset position to some extent. Therefore, it was found that the thickness of the paint thickness may significantly alter the C_p distribution.

VII.Monte Carlo based UQ for C_l with kriging surrogate model

The uncertainty quantification for aerodynamic performance (C_l) has been analyzed in this section. The convergence of the four moments are performed and shown in Fig. 15.The expected value for lift coefficient is $C_{l,E}$= 0.6376. The standard deviation converges to 0.0216; the skewness to 0.452; and the kurtosis to 5.328. As the C_l without PSP binder thickness was $C_{l,o}$ = 0.6415, a drop down of 0.0039 in C_l has been obtained due to the PSP thickness effect. The coefficient of variation for lift coefficient CoV_l=3.38%. According to the previous discussion for pressure coefficient, the drop down of C_l was consistent with the increased C_p on upper surface of airfoil before the shock due to the PSP binder thickness. The probability distribution $p_X(C_l)$ for C_l is shown in Fig. 16. Fig. 17 shows the cumulative distribution $P_X(C_l)$ for C_l with deviation, where $P_X(C_l)=\int p_X(C_l)d(C_l)$. The deviation is the difference between obtained C_l and the expected value. The probability of obtaining a C_l less than 0.6149 is 1%. The probability of obtaining a C_l less than 0.6476 is 50%. The

probability of obtaining a C_l less than 0.7041 is 99%. Therefore, the chance of having a C_l less than 0.6149 or greater than 0.7041 is 1% which can be regarded as rare event. The corresponding lower and upper bonds for deviations are respectively 0.0227 and 0.0665.

Therefore, under the effect of average PSP paint binder thickness, the lift coefficient decreased from $C_{l,o}$= 0.6415 to $C_{l,E}$ = 0.6376 deterministically. Moreover, due to the paint's random non-uniformity, C_l deviation varies from $C_{l,E}$ −0.0227 to $C_{l,E}$ +0.0665.

The Statistic moments and results were showed in Table 5. The standard deviation is 0.0216 which quantifies the amount of dispersion of the data. The distribution of $C_p$has a positive skewness that can also be found from output distribution in Fig. 16. The kurtosis value indicates the presence of infrequent extreme deviations that accounts for the "Black swan" event. The uncertainty quantification result suggests a deviation of the lift coefficient ranging from -0.0227 to +0.0665. Therefore a percentage deviation ranging from -3.5% to +10.4% was obtained by using the lower and upper bonds of deviation divided by$C_{l,E}$. As seen in the obtained results of outputs, compared with UQ for C_p, performance parameters of UQ for C_l shows a larger CoV. It can be found that the measured C_l can be under-predicted by up to 3.5% and over-predicted by up to 10.4% relative to the deterministic value with a probability of occurrence less than 0.01. For a higher chance about 10% of occurrence, the measured C_l can be under-predicted by up to 1.2% and over-predicted by up to 5.8% relative to the deterministic value.

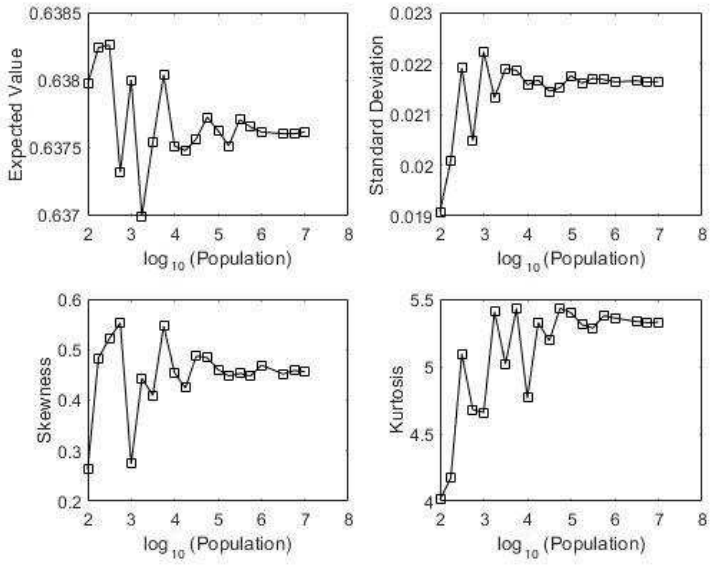

Fig. 15 Convergence of four statistic moments

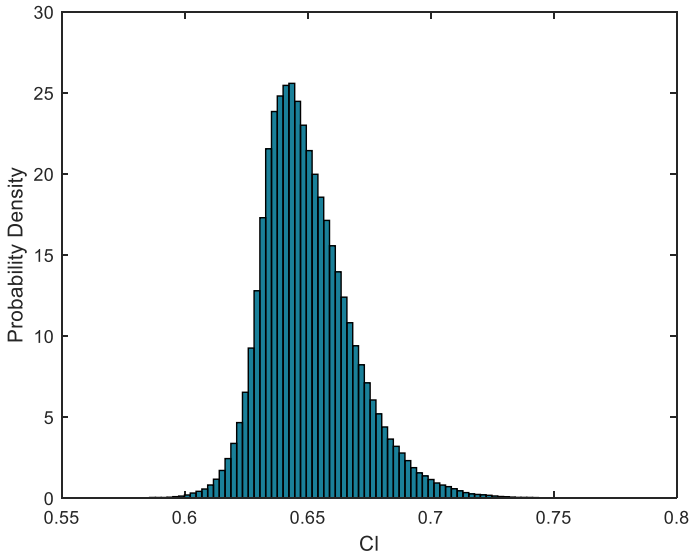

Fig. 16 Output C_l probability distribution

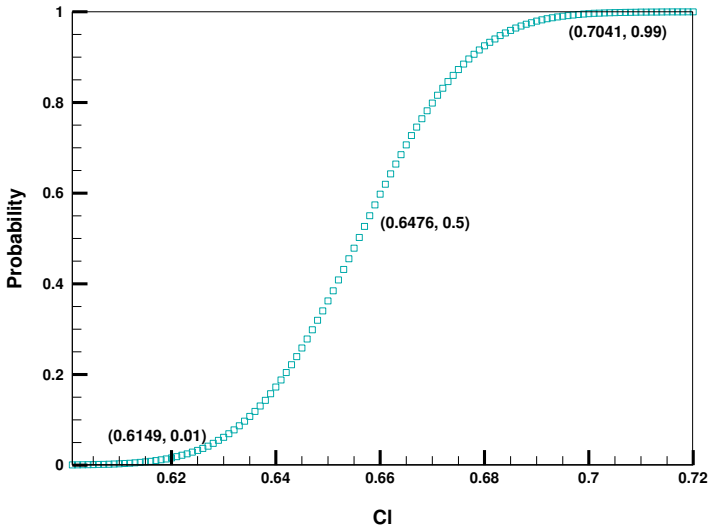

Fig. 17 Probability of obtaining deviation for lift coefficient beyond certain range

Table 5 Statistic moments and results

	Expected value	Std. deviation	Skewness	Kurtosis	C_l deterministic drop	C_l percentage deviation
Kriging	0.6376	0.0216	0.452	5.328	0.0039	-3.5%~10.4%

VIII.Conclusion

To investigate the uncertainty caused by the paint thickness in PSP measurement, a parameterization and mesh generation method has been developed to represent an NLF airfoil with small deviations on the upper surface due to the addition of the PSP binder thickness. From the results obtained via kriging surrogate model, it was found that the surrogate model can provide output values with negligible deviations from that of the flow simulations, proving the accuracy of the surrogate model. Monte Carlo simulations have been carried out with 10^7 samples of geometric uncertain variables with a CoV of 3%.

On the aerodynamic uncertainty due to thickness effect, the following conclusions can be drawn. By using the proposed surrogate model with MCM, the variation of paint thickness has been proved to be one of the reasons to account for the decrease in measured pressure ahead of the shock wave as observed in the wind tunnel PSP measurement. The uncertainty effects on measured pressure coefficient and lift coefficient have been studied. From the results we found that the small geometric shape alteration of the airfoil due to the paint thickness can lead to an increase of flow compressibility, which will in turn cause the shock forward lead and a slightly pressure increase ahead of the shock. The geometrical uncertainty will lead to errors of the measured results to some extent. The pressure coefficient shows a CoV of 0.6%, and the lift coefficient shows a CoV of 3.8%. The extreme values of scatter in lift coefficient show up to 10.4% greater and 3.5% less than the deterministic baseline value, although with a probability of occurrence of less than 1%. However, for a higher chance about 10% of occurrence, measured lift coefficient can be under-predicted by up to 1.2% and over-predicted by up to 5.8% relative to the deterministic value. This study further verified that the PSP is a high accuracy measuring technique, though considering the geometrical error due to the different paint thickness. Even for the rare event, the accuracy of the PSP is about 90%. The uncertainty quantification results provide useful bonds on measured pressure and lift coefficient in PSP measurement. The geometric uncertainties due to thickness variation can affect the measured results.

It is worth noting that this work is based on theoretical model with assumptions of input CoV. The outcome of this study clearly shows the necessity of incorporating randomness of geometric variables in the PSP measuring process of aerodynamic experiment. Shifting from deterministic point of view to uncertainty quantification, UQ allows for quantification of the effects of the uncertain geometric input on the measured aerodynamic forces acting on the airfoil with the statistical information.

Acknowledgments

The authors would like to acknowledge the support from the National Science Foundation (No. 11432007) and the Priority Academic Program Development of Jiangsu Higher Education Institutions of China for supporting the research.

References

[1] Liu, T., Pressure- and Temperature-Sensitive Paints, Encyclopedia of Aerospace Engineering, John Wiley & Sons, Ltd, 2011, pp. 9-10.

doi: 10.1002/9780470686652.eae076

[2] Ouchi, H., Irikado, T., Fujii, K., and Hayashi, A., "PSP Measurements in the Large-Scale Transonic Wind Tunnel and Associated Image Data Processing," 43rd AIAA Aerospace Sciences Meeting and Exhibit, Aerospace Sciences Meetings, Reno, Nevada, Jan. 2005, pp. 10-13.

doi: 10.2514/6.2005-1079

[3] Peng, D., Jiao, L., Sun, Z., Gu, Y., and Liu, Y., "Simultaneous PSP and TSP measurements of transient flow in a long-duration hypersonic tunnel", Experiments in Fluids, Vol. 57, No. 188, 2016.

doi: 10.1007/s00348-016-2280-z

[4] Peng, D., Wang, S., and Liu, Y., "Fast PSP measurements of wall-pressure fluctuation in low-speed flows: improvements using proper orthogonal decomposition", Experiments in Fluids, Vol. 57, No. 45, 2016.

doi: 10.1007/s00348-016-2130-z

[5] Xiang, X., Yuan, M., Yu, J., Shi, Y., Chen, L., Wang, Z., and Liu, Z., "Fast Response PSP Measurement in a Hypersonic Wind Tunnel," 30th AIAA Aerodynamic Measurement Technology and Ground Testing Conference, Atlanta, June 16-20, 2014.

doi: 10.2514/6.2014-2943

[6] Sakaue, H., and Sullivan, J., P., "Time Response of Anodized Aluminum Pressure-Sensitive Paint", *AIAA Journal*, Vol. 39, No. 10, 2001, pp. 1944-1949.

doi: 10.2514/2.1184

[7] Sajben, M., "Uncertainty Estimates for Pressure Sensitive Paint Measurements", AIAA Journal, Vol. 31, No. 11, 1993, pp. 2106-2110.

doi: 10.2514/3.11897

[8] Ruyten, W., "Full-Field Uncertainty Determination for Pressure-Sensitive Paint Measurements", AIAA Journal, Vol. 46, No. 5, 2008, pp. 1266-1268.

doi: 10.2514/1.32127

[9] Hubner, J., P., Carroll, B., F., Schanze, K., S., and Ji, H., F., "Pressure-sensitive paint measurements in a shock tube", Experiments in Fluids, Vol. 28, No. 1, 2000, pp. 21-28.

doi: 10.1007/s003480050003

[10] Liu, T., Guille, M., and Sullivan, J., P., "Accuracy of Pressure-Sensitive Paint", AIAA Journal, Vol. 39, No. 1, 2001, pp. 104-112.

doi: 10.2514/2.1276

[11] Montomoli, F., Carnevale, M., D'Ammaro, A., Massini, M., and Salvadori, S., Uncertainty Quantification in Computational Fluid Dynamics and Aircraft Engines, edited by F. Montomoli, M. Carnevale, A. D'Ammaro, M. Massini and S. Salvadori, Springer, London, 2015, pp. 33-34.

[12] DeGennaro, A. M., "Uncertainty Quantification for Airfoil Icing", Ph.D. Dissertation, the Department of Mechanical and Aerospace Engineering of Princeton University, 2016, pp. 128-133.

[13] Seshadri, P., Shahpar, S., and Parks, G., "Robust compressor blades for desensitizing operational tip clearance variations,"

Proceedings of ASME Turbo Expo 2014, Vol. 2A, Düsseldorf, Germany, June 16-20, 2014.

[14] Goodhand, M., and Miller, R., "The Impact of Real Geometries on Three-Dimensional Separations in Compressors," Journal of Turbomachinery, Vol. 134, March, 2012, pp. 021001-8.

doi: 10.1115/1.4002990

[15] Bunker, R., "The Effects of Manufacturing Tolerances on Gas Turbine Cooling," Journal of Turbomachinery, Vol. 131, October, 2009, pp. 041018-11.

doi: 10.1115/1.3072494

[16] Montomoli, F., and Massini, M., "Gas turbines and uncertainty quantification: Impact of PDF tails on UQ predictions, Black Swan." Proceeding of ASME Turbo Expo 2013: Turbine Technical Conference and Exposition GT2013, San Antonio, Texas, USA, June 3-7, 2015, GT2013-94306.

doi: 10.1115/GT2013-94306

[17] Zhu, M., Li, Y., Qin, N., Huang, Y., Deng, F., Wang, Y., and Zhao, N., "Shock Control of a Low-Sweep Transonic Laminar Flow Wing", AIAA Journal, 2018, pp. 1-13.

doi: 10.2514/1.J058011

[18] Randell, T. C. S., and Allen, C. B., "Efficient mesh motion using radial basis functions with data reduction algorithms," 46th AIAA Aerospace Sciences Meeting and Exhibit, Aerospace Sciences Meetings, Reno, Nevada, Jan. 7-10, 2008.

doi: 10.2514/6.2008-305

[19] Wang, Y., Liu, S., Qin, N., Radial Basis Function Parameterization for Airfoil, Cross-Strait Workshop of Fluid Mechanics, Xining, China, Sept, 2016.

[20] Buhmann, M., Radial Basis Functions, Acta Numerica, 2000, pp. 1-38.

doi: 10.1007/978-3-642-18754-4_3

[21] Knupp, P. M., Algebraic mesh quality metrics for unstructured initial meshes, Finite Elements in Analysis and Design, Vol.

39, 2003, pp. 217-241.

doi: 10.1016/s0168-874x(02)00070-7

[22] Yamazaki, W., and Arakawa, Y., "Numerical / Experimental Investigation of Airfoil Shape for Small VAWT", 34th Wind Energy Symposium, AIAA SciTech Forum, San Diego, California, USA, 2016.

doi: 10.2514/6.2016-1733

[23] Lophaven, S., Nielsen, H., and Søndergaard, J., "DACE A MATLAB Kriging Toolbox," Technical Report IMM TR-2002-12, DK-2800, Kgs. Lyngby, Denmark, August 2002.

[24] Siva, C. Murugan, M. S., and Ganguli, R., "Uncertainty Quantification in Helicopter Performance Using Monte Carlo Simulations", Journal of Aircraft, Vol. 48, No. 5, 2011, pp. 1503-1511.

doi: 10.2514/1.C000288

[25] Grafarend, E. W., Linear and Nonlinear Models: Fixed Effects, Random Effects, and Mixed Models, Walter de Gruyter, Berlin, 2006, Chapters. 1, 2.